

Improving Automated Detection of Cataract Disease through Transfer Learning using ResNet50

Salwa Shakir Mahmood

ATISP Research Unit National School of Electronics and Telecommunications of Sfax (ENET'Com), Sfax University, Tunisia
ank.gabor@yahoo.com (corresponding author)

Sihem Chaabouni

Centre de Recherche en Numerique de Sfax, Sfax, Sfax Technopole, Sfax University, Tunisia
sihem.chaabouni@entcom.usf.tn

Ahmed Fakhfakh

Centre de Recherche en Numerique de Sfax, Sfax, Sfax Technopole, Sfax University, Tunisia
ahmed.fakhfakh@entcom.usf.tn

Received: 26 July 2024 | Revised: 11 August 2024 | Accepted: 12 August 2024

Licensed under a CC-BY 4.0 license | Copyright (c) by the authors | DOI: <https://doi.org/10.48084/etasr.8530>

ABSTRACT

Manual diagnosis of eye diseases through ocular fundus scans is a challenging and complicated task because it is time-consuming and prone to errors. Deep learning techniques are used to detect various ocular diseases from fundus images. Such techniques can accurately classify ocular scans, enabling automated and precise detection of ocular diseases. This study uses the ResNet50 transfer learning model, data augmentation, fine-tuning, binary classification, and rigorous evaluation to achieve state-of-the-art results in the detection of cataract eye disease. This study was primarily implemented on a heavily skewed ODIR-5K dataset comprising 5000 fundus images. These ocular images are distributed unevenly among eight disease classes, including cataract, glaucoma, diabetic retinopathy, age-related macular degeneration, and others. In response to this imbalance and disparity, the proposed approach involved converting the multiclass problem into binary classification tasks, maintaining an equitable distribution of samples within each class. A balanced dataset was used to train a binary classifier using the ResNet50 CNN model. The system achieved an overall test accuracy of 96.63%, outperforming previous methods in differentiating between normal and cataract cases. In general, achieving dataset balance and employing the ResNet50 model enhances the accuracy of automated diagnosis of ocular diseases based on fundus images.

Keywords-cataract detection; classification; transfer learning; ResNet50; fundus images; fine-tuning; deep learning

I. INTRODUCTION

Ocular diseases refer to any abnormalities or visual impairments that disrupt the normal functioning of the eyes or adversely affect visual acuity [1]. Retinal disorders are the leading causes of visual impairment, encompassing other conditions such as glaucoma, cataracts, diabetic retinopathy, and age-related macular degeneration. By 2030, more than 400 million people will be affected by retinopathy [2, 3]. Swift detection of these conditions is invaluable to avoid visual loss. Screening the fundus by manual inspection is time-consuming and is highly dependent on the experience of specialist ophthalmologists. However, the prompt identification of eye diseases can benefit from automated computer-aided tools [4].

Different demographic characteristics, such as sex, age, profession, climate, hygiene, etc., play a pivotal role in the incidence of eye conditions. Many studies have revealed an increased incidence of ocular infections in tropical populations compared to temperate regions, with environmental factors such as dust, humidity, sunlight, and other contributing factors [5]. The World Health Organization (WHO) states that about 2.2 billion people worldwide have near or far vision impairment [6]. Based on projections, 50% of these cases were potentially preventable or treatable. Similarly, an estimated one billion individuals are affected by moderate to severe distance vision problems or blindness caused by uncorrected refractive errors, glaucoma, corneal opacities, cataracts, and diabetic retinopathy. Uncorrected presbyopia also contributes to near-

vision deficits in more than 800 million people [7]. These statistics show that unprivileged groups need affordable access to eye care.

There is a growing interest in using deep learning for medical imaging, with promising results in detection, classification, and medical diagnosis. Furthermore, automated disease detection can decrease the routine workload of ophthalmologists. This study seeks to classify eye diseases, using the ODIR-5K dataset, comprising 5000 fundus images, to train and test the ResNet50 deep learning framework. However, the dataset shows a significant class imbalance, making disease classification ineffective due to the instability it introduces during training. To address this concern, a binary balancing method was applied, extracting equal samples from two classes and inputting them into a pre-trained ResNet50 model. This approach focused on balanced two-class classification rather than multiclass disease classification on an entirely imbalanced dataset to improve model training and performance.

II. LITERATURE REVIEW

Many approaches have been proposed for the classification of ocular diseases. In [8], a two-stage technique was used to achieve precise optical disc localization, utilizing Convolutional Neural Networks (CNNs). In [9], ReLayNet was proposed, which used knowledge distillation models and sequential deep network training. ReLayNet functions as a fully convolutional encoder-decoder network, specifically designed for the semantic segmentation of retinal layers and fluids derived from Optical Coherence Tomography (OCT) scans [10]. In [11], a method was proposed to diagnose various retinal conditions using OCT. OCT scans were classified pixel-wise using CNNs with dilated convolution filters, and performance was assessed by analyzing 400 scans from patients with Age-related Macular Degeneration (AMD). In [12], a CNN-based method was introduced to detect intraretinal fluid on OCT scans. The CNN model was trained on a dataset comprising 1289 OCT scan images, demonstrating notable performance with a dice score of 0.911 in cross-validation.

In [13], a supervised learning technique was introduced, featuring an innovative convolutional multitask structure. The model was trained to segment bright and red lesions in fundus images. It demonstrated robust performance, achieving an impressive 0.839 Area Under the Curve (AUC) score. In [14], a novel approach was proposed to segment blood vessels in the retina through Conditional Random Fields (CRF) linked to a CNN (CRF-CNN). The performance of the CRF-CNN model was evaluated by examining its effectiveness and accuracy on color-fundus visuals from two established datasets, DRIVE and STARE [15, 16]. Similarly, in [17], an automated deep-learning technique was proposed to identify diabetic retinopathy and macular edema. This was achieved by fine-tuning a neural network image classification architecture. In [18], various retinal diseases were diagnosed from OCT visuals by employing fine-tuned CNNs, including GoogLeNet. The images were classified into three sets, namely diabetic-macular edema, dry age-linked macular degeneration, and no pathology. Visual Geometry Group 19-layer deep CNN (VGG-19) effectively detected cataracts in color fundus images,

highlighting the versatility of this model and its impact on the advancement of diagnostic capabilities. Various other research efforts have similarly delved into assessing different methods [19]. In [20], deep learning models were optimized to detect ocular diseases. These methods exemplify the continuous exploration and refinement of advanced technologies to enhance the precision and versatility of retinal disease diagnosis.

III. METHODOLOGY

This study used transfer learning with the ResNet50 neural network for cataract detection. ResNet50 is a 50-layer deep CNN for image classification, which introduced identity skip connections, allowing practical training of intense networks [21]. The dataset was selected to ensure a fair representation of each eye disease. The ODIR-5K dataset [22] includes images of various eye diseases such as diabetes, glaucoma, cataract, and AMD. The problem formulated was the binary classification between normal eyes and eyes affected by cataracts. Thus, the ODIR-5K dataset was processed to include only average and cataract images, eliminating other images that did not fit this objective. The fundus images were subsequently preprocessed and inputted into ResNet50, which can scrutinize such visual information or imagery. A series of experiments were carried out to train ResNet50 and achieve better classification results. The image dimensions were modified to improve accuracy, involving convolutional layers that extracted relevant features and decreased dimensionality. A sequential Keras model was developed using ResNet50, flattening its outputs and adding a single sigmoid-activated node to binary classify cataract or non-cataract images. The model leveraged the pre-trained features of ResNet50 to classify images with or without cataract. Figure 1 presents the proposed approach, which consists of several steps, including dataset readiness, ocular image preprocessing, DNN training, ResNet50 TL, and performance evaluation. Data were explored to analyze the dataset, by examining the details of the initial five patient records to develop an initial understanding of the characteristics and data structure.

A. ODIR-5k Dataset

This dataset consists of color fundus visuals of both the left and right eyes from 5,000 patients. Doctor-provided diagnostic keywords and age information are included for each patient [3]. Shang-gong Medical Technology collected a dataset of 5000 patients' left and right fundus ocular visuals from various hospitals. Metadata, including patient age, sex, and diagnostic descriptors, are incorporated in labels. This ocular disease dataset, featuring eight classes of eye diseases, includes multiple conditions in individual patients, making it a multiclass and multilabel dataset. Classes include standard, glaucoma, diabetes, AMD, cataract, hypertension, and myopia. Figure 2 shows fundus images with various ophthalmological disease pathologies: (a) Devoid of any retinal abnormality, (b) glaucoma that induces damage to the optic nerve leading to increased cupping and brightness in the optic disc, (c) Diabetic retinopathy manifesting as microaneurysms, hemorrhages, and exudates, presented as distinctive red and yellow spots, (d) AMD that results in neovascularization and geographic atrophy within the retina, (e) Myopia that contributes to the thinning of

the retinal pigment epithelium, leading to peripapillary, and (f) Hypertension that causes alterations in vessel morphology, characterized by narrowed arterioles and AV nicking. Fundus imaging offers a powerful tool for noninvasive screening of

multiple ocular diseases. This is achieved by detecting characteristic morphological changes in both the retina and the optic disc.

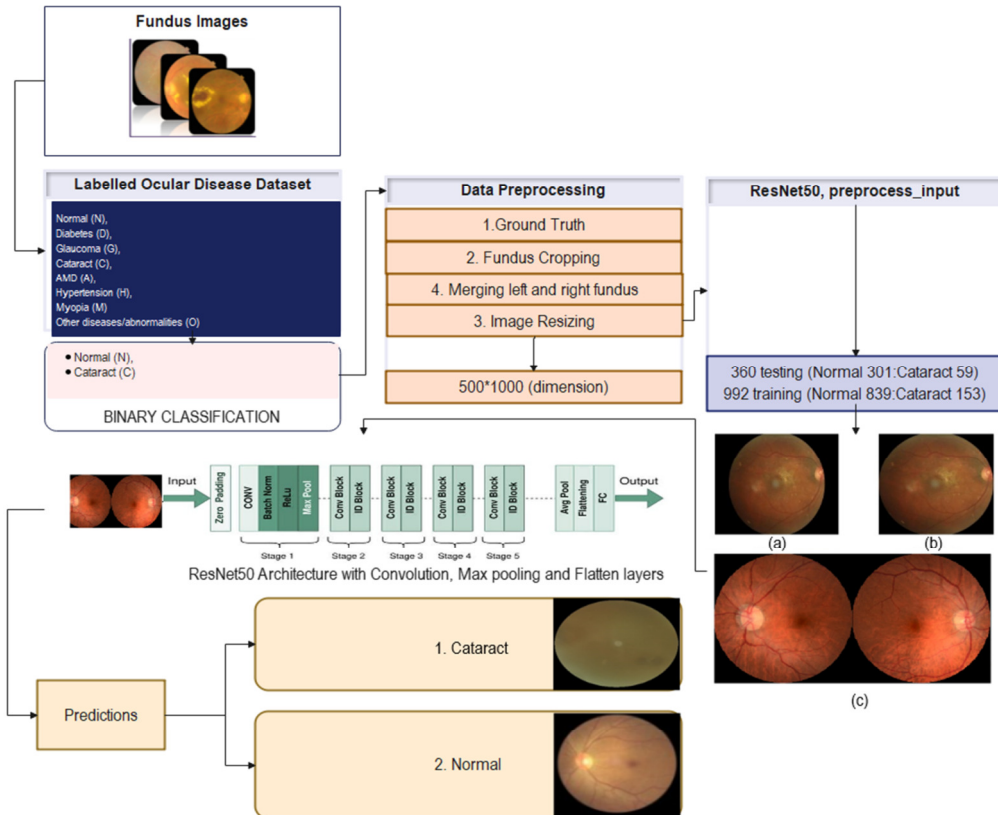


Fig. 1. System workflow. Images: (a) Original, (b) Cropped, and (c) Left and Right fundus merged.

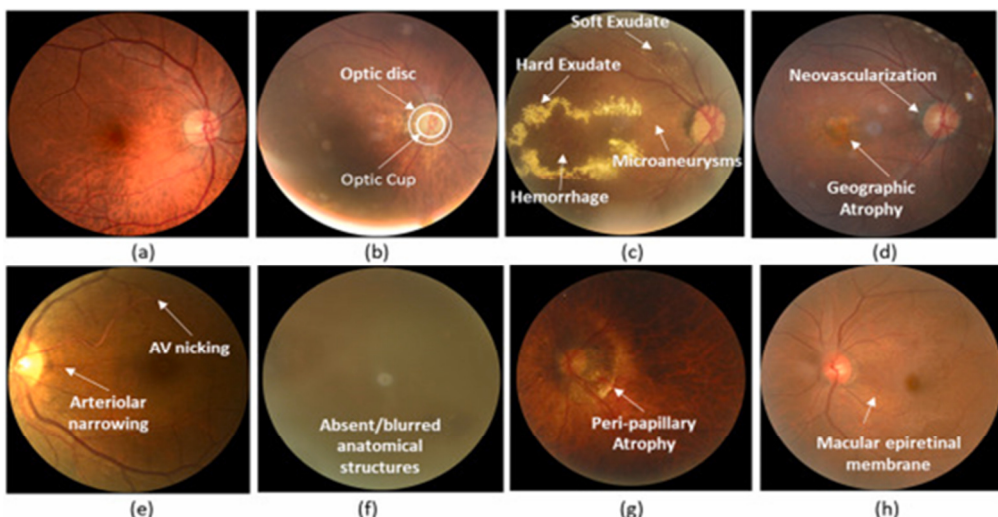


Fig. 2. Fundus-images: standard visuals.

B. Data Preprocessing

The dataset contains images of different sizes and shapes, including rectangular and triangular images. Image dimensions

vary, with sizes such as 3456×188, 5188×250, and others. This diversity is attributed to using different cameras and settings during image capture. Preprocessing steps were applied to

normalize the dataset. Black borders were removed and a combination of cropping and resizing was applied to transform the images into rectangular shapes. The left and right fundus images were merged into a single composite image.

After excluding low-quality images based on expert annotation, 1094 were chosen for further analysis. As most fundus images encompass non-informative black borders, preserving them would increase negative sample proportions and compromise diagnostic lesion detection accuracy. As a result, an automated cropping process was used. The images were segmented, distinguishing between background and

foreground components. The region containing pathological features within the foreground was then precisely identified, and the image dimensions were subsequently adjusted based on the position and dimensions of the foreground. This cropping normalized images to 1000×500 pixels, removing extraneous information and improving feature representation. Normalization also aimed to re-scale all images to streamline network optimization by standardizing the input data range. Data were distributed in a 70/30 ratio for training and testing. Figure 3 shows the fundus images before and after applying the ResNet50 preprocess_input() function.

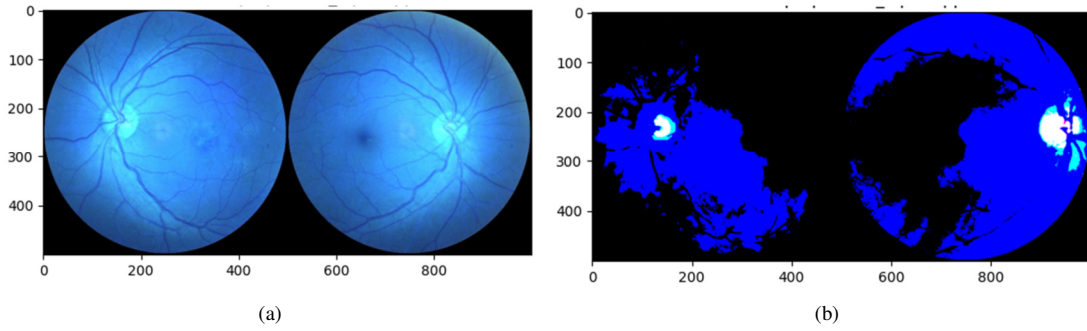


Fig. 3. Before and after applying ResNet50 preprocess_input().

C. Transfer Learning and ResNet50

In [23], CNNs were introduced to recognize handwritten digits. CNNs perform convolution operations rather than matrix multiplication, resulting in superior performance in various medical imaging tasks, including segmentation, enhancement, and classification [24, 25]. CNNs encompass various layers, including convolutional layers, batch normalization, and Rectified Linear Unit (ReLU) activation. Additionally, pooling and fully connected layers are integral components of this architecture. Collectively, these diverse layers contribute to their effectiveness in handling complex visual data. This network design has proven particularly advantageous for tasks involving medical image analysis. CNN variants, such as ResNet [26], AlexNet [27], MobileNet [28], GoogleNet [29], and VGGNet [8] have been proposed for image classification. However, these architectures demand extensive datasets to address complex challenges and attain optimal performance. Transfer learning uses information from already trained models on big datasets, such as ImageNet, to avoid the complex and time-consuming job of collecting lots of labeled data. This way, existing CNN architectures can be used for medical imaging without needing much specific medical data [29]. This study focused specifically on ResNet50 to classify fundus images. This architecture was used with Keras on TensorFlow.

D. ResNet50 Model Configuration

The ODIR-5K dataset [22] includes fundus images for both eyes of each patient. The ultimate label characterizes the image as normal or depicting a cataract. To normalize data, images were resized to 500×1000×3 using the ResNet50 preprocess_input() function. Both the left and right eyes were combined and used as input to the ResNet50 model. CNN

feature maps were pooled globally. The resulting feature vector was optimized using the sigmoid activation function, which constrains feature predictions in the range of (0, 1) [30-31]:

$$f(s) = \frac{1}{1+e^{-s}} \quad (1)$$

The sigmoid activation function calculates the likelihood of individual labels independently. If the probability is higher than 0.5, it is marked as having cataract, otherwise, it is considered normal. The Mean Squared Logarithmic Error (MSLE) loss function measures how much the predicted values differ from the actual values for both normal and cataract categories. The ResNet-50 model employs a distinctive CNN architecture that includes residual blocks with identity shortcut connections, where each block contains multiple convolutional layers using 3×3 filters and stride-2 convolutions. This architecture captures complex hierarchical features from the data while reducing reliance on excessive hyperparameters, thus contributing to its effectiveness in various computer vision tasks. This Keras sequential model leverages transfer learning from a trained ResNet50 model for feature extraction. ResNet50 provides powerful hierarchical visual representations. The model comprises the pre-trained ResNet50 base, which outputs 2048 feature maps. These feature maps are flattened to a 1D vector by a flattened layer. Finally, a single dense layer with sigmoid activation is added for binary classification. Overall, the model architecture enables efficiently use of the representation capability of the ResNet50 CNN through transfer learning, training only a tiny classifier layer on top.

IV. IMPLEMENTATION

A. Experimental Setup

Python PyCharm community edition 2021.3.2 was used for the experiments. The Adam optimizer was used with a learning rate set at 0.0003. The loss function calculation employed MSLE. A batch size of 32 was used to train the model. The training process iterated over 20 epochs. Table I shows the model summary.

TABLE I. RESNET50 TRAINING DETAILS

Data augmentation	No
Transfer learning	Yes
Weights	Pre-trained on ImageNet
Last layer	Dense (1, activation: sigmoid)
Feature extraction enabled	Yes
Classification enabled	Yes
Optimizer	Adam
Loss function	MSLE
Early stopping patience	No

B. Evaluation Metrics

Accuracy is used to measure the prediction performance of a model. However, in cases where classes are unevenly distributed, more than accuracy is needed to give a complete picture of the model's success. The F1 score is essential, as it considers both precision and recall, providing a balanced measure that accounts for false positives and negatives. Combining the F1 score with accuracy provides a more comprehensive evaluation of the model's performance, especially in situations with asymmetric class distribution or when equal importance is needed for false positives and false negatives.

$$\text{Accuracy} = \frac{(TP + TN)}{(TP + FP + FN + TN)} \quad (2)$$

with TP representing cases with accurate positive predictions, TN representing situations where predictions and actual outcomes are adverse, FP representing the number of cases that

the model predicts as positive for negative cases, and FN representing the number of positive instances that are incorrectly predicted as negative. Precision shows how well the model accurately identifies positive instances among all the positive cases. Higher precision indicates the model's ability to reduce FP predictions. Recall measures the effectiveness of a model in correctly identifying positive samples in a dataset. A higher recall indicates that the model is better at capturing TPs and fewer FN. Using recall as a single metric makes model comparisons easier, especially in domains such as cancer prediction, where overlooking true positives can have severe consequences. Therefore, models that maximize recall are essential.

$$\text{Precision} = \frac{TP}{(TP + FP)} \quad (3)$$

$$\text{Recall} = \frac{TP}{(TP+FN)} \quad (4)$$

$$\text{F1-score} = 2 \frac{\text{Precision} \times \text{Recall}}{(\text{Precision} + \text{Recall})} \quad (5)$$

V. RESULTS AND DISCUSSION

The ResNet50 model was trained for 20 epochs in the cataract image dataset. The training process involved optimization of the model's parameters to minimize loss and improve the accuracy of both the training and validation data. Throughout 20 epochs, the model consistently improved performance, with the training loss decreasing and the training accuracy increasing. Similarly, the validation loss trended downward and validation accuracy improved over the training process. The gap between the training and validation metrics was small, indicating that the model did not overfit the training data. Figure 4 shows an accuracy and loss plot for both training and testing of the model. After 20 epochs, the model achieved a high level of performance in both training and validation data. An overall test accuracy of 96.63% was achieved. The difference in error between the training and testing data was negligible (0.0001634), suggesting that the model could generalize well to unseen data.

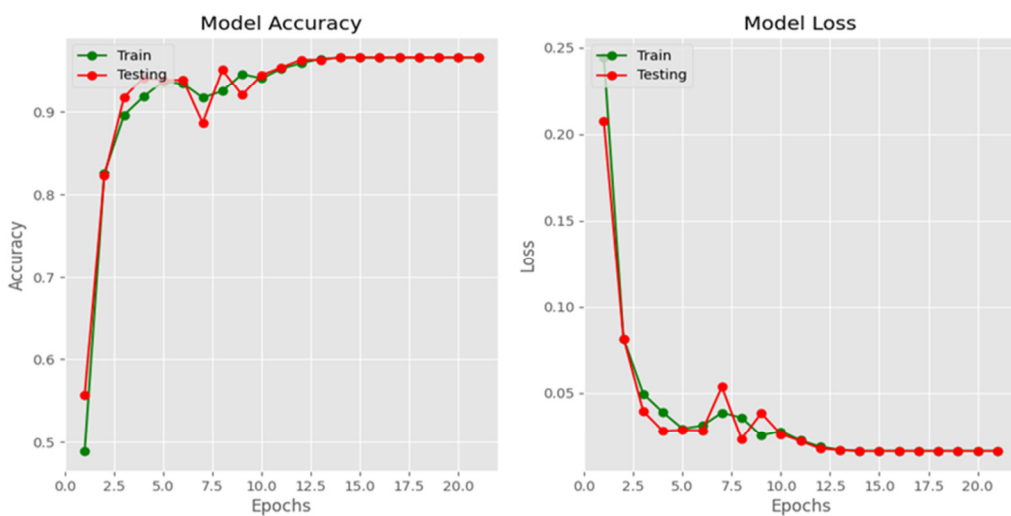


Fig. 4. Accuracy and loss plots on both training and testing phases.

When evaluated in the test set, the model demonstrated strong performance, accurately predicting most normal and cataract images. Table II shows in detail the evaluation metrics of the proposed model in the testing phase.

TABLE II. EVALUATION RESULTS

Testing Details	Value
Testing Accuracy	0.9663
Testing Loss	0.0162
Testing Recall	0.9661
Testing Precision	0.9715
Testing AUC	0.9661

VI. CONCLUSION AND FUTURE WORK

This study used ResNet50, a CNN-based deep learning model, to detect whether an eye fundus is normal or has a cataract. The model performed very well, exceeding expectations, as it achieved 96.58% training accuracy and 96.63% testing accuracy. The proposed approach outperformed current CNN models in terms of accuracy while demanding reduced latency. When comparing different studies in this field, it is worth mentioning the significant findings of [32], which used a specifically constructed CNN model and achieved a test accuracy of 94.2% in classifying normal vs. cataract cases on the ODIR-5K dataset. In [30], a transfer learning technique using VGG-16 achieved a test accuracy of 95.8% on the same dataset for binary classification. Furthermore, in [31], ResNet50 obtained an average accuracy of 93.5% on the same dataset.

In addition, the proposed method can be easily adapted for other medical image classification tasks. The ResNet50 model is promising for real-world ocular disease diagnosis systems. One notable benefit is its versatility for other medical image classifications. This model demonstrates significant potential to assist medical professionals and revolutionize ocular disease screening. However, further research is required to enhance accuracy, especially in cases of glaucoma. Despite this, the current results are promising and, with additional data and experimentation, could evolve into a highly effective disease classification tool. In addition, future studies can combine the proposed method with [33-38] to obtain better transmission and signal processing.

REFERENCES

- [1] B. Trstenjak, D. Donko, and Z. Avdagic, "Adaptable Web Prediction Framework for Disease Prediction Based on the Hybrid Case Based Reasoning Model," *Engineering, Technology & Applied Science Research*, vol. 6, no. 6, pp. 1212–1216, Dec. 2016, <https://doi.org/10.48084/etasr.753>.
- [2] A. O. Adio, A. Alikor, and E. Awoyesuku, "Survey of pediatric ophthalmic diagnoses in a teaching hospital in Nigeria," *Nigerian journal of medicine*, vol. 20, no. 1, pp. 105–108, Jan. 2011.
- [3] N. Li, T. Li, C. Hu, K. Wang, and H. Kang, "A Benchmark of Ocular Disease Intelligent Recognition: One Shot for Multi-disease Detection," in *Benchmarking, Measuring, and Optimizing*, 2021, pp. 177–193, https://doi.org/10.1007/978-3-030-71058-3_11.
- [4] Y. Elloumi, M. Akil, and H. Boudeggaa, "Ocular diseases diagnosis in fundus images using a deep learning: approaches, tools and performance evaluation," in *Real-Time Image Processing and Deep Learning 2019*,
- [5] P. Paudel *et al.*, "Prevalence of vision impairment and refractive error in school children in Ba Ria – Vung Tau province, Vietnam," *Clinical & Experimental Ophthalmology*, vol. 42, no. 3, pp. 217–226, 2014, <https://doi.org/10.1111/ceo.12273>.
- [6] "Blindness and vision impairment," *World Health Organization*. <https://www.who.int/news-room/fact-sheets/detail/blindness-and-visual-impairment>.
- [7] J. D. Steinmetz, "Causes of blindness and vision impairment in 2020 and trends over 30 years, and prevalence of avoidable blindness in relation to VISION 2020: the Right to Sight: an analysis for the Global Burden of Disease Study (vol 2, pg 144, 2021)," *Lancet Global Health*, vol. 9, no. 4, 2021.
- [8] K. Simonyan and A. Zisserman, "Very Deep Convolutional Networks for Large-Scale Image Recognition," *arXiv*, Apr. 10, 2015, [Online]. Available: <http://arxiv.org/abs/1409.1556>.
- [9] X. Meng, X. Xi, L. Yang, G. Zhang, Y. Yin, and X. Chen, "Fast and effective optic disk localization based on convolutional neural network," *Neurocomputing*, vol. 312, pp. 285–295, Oct. 2018, <https://doi.org/10.1016/j.neucom.2018.05.114>.
- [10] C. S. Lee, A. J. Tyring, N. P. Deruyter, Y. Wu, A. Rokem, and A. Y. Lee, "Deep-learning based, automated segmentation of macular edema in optical coherence tomography," *Biomedical Optics Express*, vol. 8, no. 7, pp. 3440–3448, Jul. 2017, <https://doi.org/10.1364/BOE.8.003440>.
- [11] C. Playout, R. Duval, and F. Cheriet, "A Novel Weakly Supervised Multitask Architecture for Retinal Lesions Segmentation on Fundus Images," *IEEE Transactions on Medical Imaging*, vol. 38, no. 10, pp. 2434–2444, Jul. 2019, <https://doi.org/10.1109/TMI.2019.2906319>.
- [12] H. C. Shin *et al.*, "Deep Convolutional Neural Networks for Computer-Aided Detection: CNN Architectures, Dataset Characteristics and Transfer Learning," *IEEE Transactions on Medical Imaging*, vol. 35, no. 5, pp. 1285–1298, Feb. 2016, <https://doi.org/10.1109/TMI.2016.2528162>.
- [13] K. Hu *et al.*, "Retinal vessel segmentation of color fundus images using multiscale convolutional neural network with an improved cross-entropy loss function," *Neurocomputing*, vol. 309, pp. 179–191, Oct. 2018, <https://doi.org/10.1016/j.neucom.2018.05.011>.
- [14] J. Staal, M. D. Abramoff, M. Niemeijer, M. A. Viergever, and B. van Ginneken, "Ridge-based vessel segmentation in color images of the retina," *IEEE Transactions on Medical Imaging*, vol. 23, no. 4, pp. 501–509, Apr. 2004, <https://doi.org/10.1109/TMI.2004.825627>.
- [15] Z. Li, Y. He, S. Keel, W. Meng, R. T. Chang, and M. He, "Efficacy of a Deep Learning System for Detecting Glaucomatous Optic Neuropathy Based on Color Fundus Photographs," *Ophthalmology*, vol. 125, no. 8, pp. 1199–1206, Aug. 2018, <https://doi.org/10.1016/j.ophtha.2018.01.023>.
- [16] V. Gulshan *et al.*, "Development and Validation of a Deep Learning Algorithm for Detection of Diabetic Retinopathy in Retinal Fundus Photographs," *JAMA*, vol. 316, no. 22, pp. 2402–2410, Dec. 2016, <https://doi.org/10.1001/jama.2016.17216>.
- [17] M. S. M. Khan, M. Ahmed, R. Z. Rasel, and M. M. Khan, "Cataract Detection Using Convolutional Neural Network with VGG-19 Model," in *2021 IEEE World AI IoT Congress (AIoT)*, Seattle, WA, USA, May 2021, pp. 0209–0212, <https://doi.org/10.1109/AIoT52608.2021.9454244>.
- [18] T. Guergueb and M. A. Akhloufi, "Ocular Diseases Detection using Recent Deep Learning Techniques," in *2021 43rd Annual International Conference of the IEEE Engineering in Medicine & Biology Society (EMBC)*, Nov. 2021, pp. 3336–3339, <https://doi.org/10.1109/EMBC46164.2021.9629763>.
- [19] H. S. Gill and B. S. Khehra, "Fruit Image Classification using Deep Learnin," Research Square, 2022, <https://doi.org/10.21203/rs.3.rs-574901/v1>.
- [20] X. Luo, J. Li, M. Chen, X. Yang, and X. Li, "Ophthalmic Disease Detection via Deep Learning With a Novel Mixture Loss Function," *IEEE Journal of Biomedical and Health Informatics*, vol. 25, no. 9, pp. 3332–3339, Sep. 2021, <https://doi.org/10.1109/JBHI.2021.3083605>.

- [21] D. Checkedath and R. R. Sedamkar, "Detecting Affect States Using VGG16, ResNet50 and SE-ResNet50 Networks," *SN Computer Science*, vol. 1, no. 2, Mar. 2020, Art. no. 79, <https://doi.org/10.1007/s42979-020-0114-9>.
- [22] "Ocular Disease Intelligent Recognition ODIR-5K," *Academic Torrents*. <https://academictorrents.com/details/cf3b8d5ecdd4284eb9b3a80fcfe9b1d621548f72>.
- [23] Y. Lecun, L. Bottou, Y. Bengio, and P. Haffner, "Gradient-based learning applied to document recognition," *Proceedings of the IEEE*, vol. 86, no. 11, pp. 2278–2324, Aug. 1998, <https://doi.org/10.1109/5.726791>.
- [24] N. Gour and P. Khanna, "Multi-class multi-label ophthalmological disease detection using transfer learning based convolutional neural network," *Biomedical Signal Processing and Control*, vol. 66, Apr. 2021, Art. no. 102329, <https://doi.org/10.1016/j.bspc.2020.102329>.
- [25] K. He, X. Zhang, S. Ren, and J. Sun, "Deep Residual Learning for Image Recognition," in *2016 IEEE Conference on Computer Vision and Pattern Recognition (CVPR)*, Las Vegas, NV, USA, Jun. 2016, pp. 770–778, <https://doi.org/10.1109/CVPR.2016.90>.
- [26] A. Krizhevsky, I. Sutskever, and G. E. Hinton, "ImageNet classification with deep convolutional neural networks," *Commun. ACM*, vol. 60, no. 6, pp. 84–90, Feb. 2017, <https://doi.org/10.1145/3065386>.
- [27] A. G. Howard *et al.*, "MobileNets: Efficient Convolutional Neural Networks for Mobile Vision Applications." arXiv, Apr. 16, 2017, <https://doi.org/10.48550/arXiv.1704.04861>.
- [28] C. Szegedy *et al.*, "Going deeper with convolutions," in *Proceedings of the IEEE conference on computer vision and pattern recognition*, 2015.
- [29] A. Ng, "Nuts and bolts of building AI applications using Deep Learning," *NIPS Keynote Talk*, vol. 64, 2016.
- [30] C. Lam, C. Yu, L. Huang, and D. Rubin, "Retinal Lesion Detection With Deep Learning Using Image Patches," *Investigative Ophthalmology & Visual Science*, vol. 59, no. 1, pp. 590–596, Jan. 2018, <https://doi.org/10.1167/iovs.17-22721>.
- [31] D. S. W. Ting *et al.*, "Development and Validation of a Deep Learning System for Diabetic Retinopathy and Related Eye Diseases Using Retinal Images From Multiethnic Populations With Diabetes," *JAMA*, vol. 318, no. 22, pp. 2211–2223, Dec. 2017, <https://doi.org/10.1001/jama.2017.18152>.
- [32] A. B. Triyadi, A. Bustamam, and P. Anki, "Deep Learning in Image Classification using VGG-19 and Residual Networks for Cataract Detection," in *2022 2nd International Conference on Information Technology and Education (ICIT&E)*, Malang, Indonesia, Jan. 2022, pp. 293–297, <https://doi.org/10.1109/ICITE54466.2022.9759886>.
- [33] S. I. Yahya *et al.*, "A New Design Method for Class-E Power Amplifiers Using Artificial Intelligence Modeling for Wireless Power Transfer Applications," *Electronics*, vol. 11, no. 21, Jan. 2022, Art. no. 3608, <https://doi.org/10.3390/electronics11213608>.
- [34] S. Roshani *et al.*, "Design of a Compact Quad-Channel Microstrip Diplexer for L and S Band Applications," *Micromachines*, vol. 14, no. 3, Mar. 2023, Art. no. 553, <https://doi.org/10.3390/mi14030553>.
- [35] H. A. Hussein, Y. S. Mezaal, and B. M. Alameri, "Miniaturized Microstrip Diplexer Based on FR4 Substrate for Wireless Communications," *Elektronika ir Elektrotechnika*, vol. 27, no. 5, pp. 34–40, Oct. 2021, <https://doi.org/10.5755/j02.eie.28942>.
- [36] Y. S. Mezaal and S. F. Abdulkareem, "New microstrip antenna based on quasi-fractal geometry for recent wireless systems," in *2018 26th Signal Processing and Communications Applications Conference (SIU)*, Izmir, Turkey, May 2018, pp. 1–4, <https://doi.org/10.1109/SIU.2018.8404727>.
- [37] A. R. Azeez *et al.*, "UWB Tapered-Slot Patch Antenna with Reconfigurable Dual Band-Notches Characteristics," *Journal of Mechanics of Continua and Mathematical Sciences*, vol. 19, no. 3, pp. 40–50, Mar. 2024, <https://doi.org/10.26782/jmcms.2024.03.00003>.
- [38] K. S. Yamuna, M. Sugumaran, A. Arthi, and R. Premkumar, "Design and Analysis of Intrusion Detection System Using Machine Learning in Smart Healthcare System," *Journal of Mechanics of Continua and Mathematical Sciences*, vol. 19, no. 7, pp. 17–27, Jul. 2024, <https://doi.org/10.26782/jmcms.2024.07.00002>.